

Article

On the Size Discrepancies between Datasets from China Meteorological Administration and Joint Typhoon Warning Center for the Northwestern Pacific Tropical Cyclones

Jinhe Li ¹, Yubin Li ^{1,*}  and Jie Tang ²

¹ School of Atmospheric Physics, Nanjing University of Information Science and Technology, Nanjing 210044, China; 20211203019@nuist.edu.cn

² Shanghai Typhoon Institute, China Meteorological Administration, Shanghai 200030, China; tangj@typhoon.org.cn

* Correspondence: liyubin@nuist.edu.cn

Abstract: This study analyzes the Northwestern Pacific tropical cyclone (TC) size difference between the China Meteorological Administration (CMA) dataset and the Joint Typhoon Warning Center (JTWC) dataset. The TC size is defined by the near-surface 34-knot wind radius (R34). Although there is a high correlation (correlation coefficient of 0.71) between CMA and JTWC R34 values, significant discrepancies are still found between them. The JTWC tends to report larger R34 values than the CMA for large-sized TCs, while the trend is reversed for compact TCs. Despite spatial distribution discrepancies, both datasets exhibit significant similarity (spatial correlation coefficient of 0.61), particularly in latitudinal distribution; higher R34 values are observed near 25° N. An investigation of key parameters affecting R34 estimations shows that the discrepancies in R34 values between the two agencies' estimates of TC size are primarily influenced by the size itself and latitude. There is a high correlation between R34 difference and R34 values, with a high correlation of up to 0.58 with the JTWC's R34 values. There is also a significant correlation between R34 difference and latitude, with a correlation coefficient of 0.26 in both the CMA and JTWC datasets. Case studies of Typhoons "Danas" and "Maysak" confirm distinct characteristics in R34 estimations during different development stages, with the JTWC capturing TC intensification better, while the CMA underestimates TC size during rapid growth phases. During the weakening stage of the TC, both agencies accurately estimate the R34 values. These findings contribute valuable insights into the discrepancies and characteristics of R34 datasets, informing the selection and utilization of data for typhoon research and forecasting.

Keywords: tropical cyclone size; data comparison; statistical characteristics



Citation: Li, J.; Li, Y.; Tang, J. On the Size Discrepancies between Datasets from China Meteorological Administration and Joint Typhoon Warning Center for the Northwestern Pacific Tropical Cyclones. *Atmosphere* **2024**, *15*, 355. <https://doi.org/10.3390/atmos15030355>

Academic Editor: Corene Matyas

Received: 12 February 2024

Revised: 4 March 2024

Accepted: 11 March 2024

Published: 14 March 2024



Copyright: © 2024 by the authors. Licensee MDPI, Basel, Switzerland. This article is an open access article distributed under the terms and conditions of the Creative Commons Attribution (CC BY) license (<https://creativecommons.org/licenses/by/4.0/>).

1. Introduction

Tropical cyclones (TCs) are warm-core vortex systems that form over tropical oceans. They can bring about disastrous weather conditions such as strong winds, heavy rainfall, giant waves, and storm surges when they make landfall, resulting in significant human casualties and economic losses in coastal areas [1–3]. TCs have the most significant impact on three global oceanic regions, namely the Northwestern Pacific (WNP) (including the South China Sea), the North Atlantic (including the Caribbean Sea and the Gulf of Mexico), and the Indian Ocean (including the Bay of Bengal). The size of a TC is a crucial parameter strongly related to the damage caused by TCs [4]. Chan et al. [5] investigate the interannual variations in TC size in the Northwestern Pacific from 1999 to 2002, using wind data from QuikSCAT. This study finds that the average TC size increased during this period, with sizes in 1999 and 2000 being smaller compared to those in 2001 and 2002. The differences in environmental flow patterns associated with TC tracks and formation positions within these years explain the observed size changes. Kimball et al. [6] utilized the Extended Best Track (EBT) dataset, which integrates information from the tropical cyclone best-track dataset

with measurements of tropical cyclone “size parameters”. Their latest updated dataset was used to establish a size parameter climatology for North Atlantic tropical cyclones from 1988 to 2002. The study of tropical cyclone size has garnered growing attention in academic research. The WNP is one of the regions with the highest occurrence of TCs globally, accounting for approximately one third of the world’s total [7]. Given the high occurrence of TCs in the WNP and their significant impact on the region, gaining a deeper understanding of the characteristics of TC sizes becomes crucial. This understanding can enhance the prediction and monitoring capabilities of TC activities, which is paramount for mitigating disaster risks, improving disaster response capabilities, and safeguarding human lives and property in the affected regions.

In TC-warning centers in various countries, the TC size is typically determined by the maximum radial extent of critical wind speed thresholds, such as 30, 34, and 50 kn wind radii (hereafter R30, R34, R50, respectively) [8]. The TC sizes can vary greatly. For instance, R34 can range from as small as 100 km to exceeding 2200 km for different TCs [9]. Currently, different TC-warning centers have released their own TC-size datasets based on various observation data and methods. For instance, at the Joint Typhoon Warning Center (JTWC), numerous scatterometers such as QuikScat [10], the windSat, Oceansat-2, and the Advanced Scatterometer (ASCAT) [11] are used for post-season subjective and objective reanalysis of wind radii [12–14]. Since 2001, the JTWC has released the TC wind radii dataset, including the average azimuthal radii for 34, 50, and 64 kn surface winds (R34, R50, and R64, respectively) [10–17]. On the other hand, in the Regional Specialized Meteorological Center (RSMC) Tokyo, the TC wind radii dataset including R30 and R50 is determined using a comprehensive set of available observations, encompassing Himawari-8 satellite images, radar data, surface synoptic observations, ship and buoy reports, as well as ASCAT data [18]. In the Korea Meteorological Administration (KMA), the post-season analysis of wind radii primarily relies on direct estimates derived from satellite observations such as ASCAT, Multiplatform Tropical Cyclone Surface Wind Analysis (MTCSWA) [19], and Microwave Radiometers [20]. When these specific datasets are unavailable, the KMA resorts to indirectly estimating TC wind radii. This is accomplished through a regression analysis between wind radii and Vmax using KMA infrared satellite data, as described by Kwon [21] and further elaborated upon by Lee and Kwon [22].

Inconsistencies can occur in the TC size datasets released by different agencies due to the various methodologies employed [12–15]. For the WNP region, for instance, Song and Klotzbach [23] found significant discrepancies in wind radius estimates between the RSMC Tokyo and JTWC datasets. Kim et al. [24] further compared estimates of gale-force wind radii (R30 or R34) and storm-force wind radii (R50) of TCs in the WNP by the KMA and the JTWC and found that the discrepancies between the two agencies seem to be primarily determined by whether the agency estimates wind radii based only on a TC’s winds or on TC winds combined with other mid-latitude synoptic systems.

The CMA constructed an objective TC size dataset in the WNP based on the correlation between TC size and brightness temperature distribution by incorporating HURSAT data and satellite imageries from GOES, MET, GMS, MTS, and FY2 [25], and a continuous dataset from 2001 to 2016 on the WNP TC size was established. However, how the wind radius estimates of the CMA and JTWC differ and whether they have unique characteristics have yet to be evaluated. Therefore, this study aims to investigate the characteristics of R34 estimated by two agencies. The objectives include examining the correlation between the two datasets, analyzing their spatial distribution characteristics, and studying the variations in their R34 discrepancies. After conducting a systematic statistical analysis of the discrepancies between the two datasets, a case comparison study is performed using the ASCAT dataset. This additional analysis aims to reveal more detailed characteristics of the two datasets. The flow diagram of this study is shown in Figure 1. The rest of this paper is organized as follows. Section 2 describes the data and methods used. Section 3 compares R34 estimates between the two agencies. The final section summarizes the results and concludes this paper.

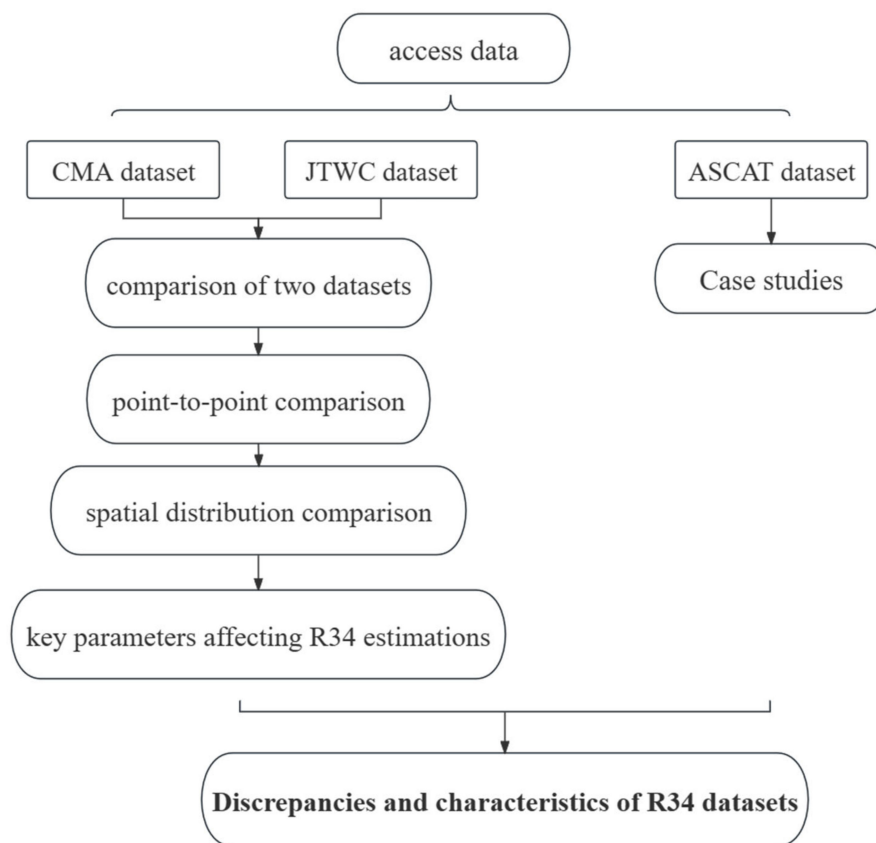


Figure 1. Flow diagram.

2. Data and Methods

2.1. Datasets

2.1.1. CMA TC Size Datasets

The CMA TC size data, obtained from the China Meteorological Administration, include all TCs in the WNP that were captured by satellites (<http://www.tcddata.typhoon.org.cn>, accessed on 20 December 2022) [25]. The spatial coverage extends north of the equator and west of 180°, including the South China Sea. The dataset provides TC size every 6 h from 2001 to 2016. Samples below tropical storm level (with a maximum 10 m above surface level wind speed near the center of 17.2 m/s) were excluded. The CMA data primarily employ a 2 min average wind speed to record the maximum 10 m above-surface-level wind speed near the center.

2.1.2. JTWC TC Size Datasets

The data from JTWC were obtained from the Joint Typhoon Warning Center (<https://www.metoc.navy.mil/jtwc/jtwc.html?western-pacific>, accessed on 20 December 2022). The best track data of JTWC encompass information about TC location, intensity, and wind radius at 6 h intervals. Typically, the JTWC records the maximum 10 m above-surface-level wind speed using a 1 min average wind speed. The time frame of the data used in this study ranged from 2001 to 2016. The four-quadrant R34 data (northeast, southeast, southwest, and northwest) from the JTWC were averaged to obtain the average R34 data.

2.1.3. ASCAT Datasets

The ASCAT data utilized for TC size validation in this study were obtained from the Royal Netherlands Meteorological Institute (KNMI) (<http://www.knmi.nl/scatterometer/ascatsi12prod/>, accessed on 15 July 2022). This dataset was collected by the Satellite Application Facilities (SAF) of the European Organisation for the Exploitation of Meteorological Satellites (EUMETSAT). The wind speed was retrieved using the geophysi-

cal model function (GMF), specifically CMOD5.n, and the maximum likelihood estimator (MLE) method. A two-dimensional variational ambiguity removal (2D-VAR) technique was employed to eliminate wind direction ambiguity and generate the final wind field product.

2.2. Data Preprocessing

Due to differences in wind speed definitions between the CMA and JTWC, comparing the R34 values poses challenges. However, sensitivity experiments involving the conversion of data to a specific wind speed definition indicate that the impact of this difference is relatively small. Yu et al. [26] proposed that the CMA established a linear relationship between 1 min and 10 min average wind speeds using an empirical formula, multiplying the average wind speed by 0.871. The assumed application of a 10 min average definition in the CMA dataset is supported by findings of relatively small differences among the JMA and CMA [13]. Therefore, following Yu et al. [26], the 1 min average wind speed of the JTWC was converted to the 10 min average wind speed for better comparison.

Besides the difference in averaging time, the TC center positions differ between the two datasets. In this case, we only considered cases where the distance between their centers is less than or equal to 0.5° . This maximum difference of 0.5° was chosen to ensure that most of the data were included. Applying this criterion, a total of 4795 data points were retained. This accounted for 79.3% of the original 6050 data points in the CMA dataset and 70.6% of the 6791 data points in the JTWC dataset.

2.3. Method for Estimating R34 Using Satellite Data

This study utilized the method proposed by Chan [19] to calculate R34 using satellite data. The methodology involves averaging winds within each 0.25° latitude-wide belt (the radial area of the first belt ranging from 0.125° to 0.375° latitude) to obtain azimuthally averaged winds between 0.25° and 6.25° latitudes relative to the TC center. The application of azimuthal averaging aims to mitigate the asymmetry associated with TC movement [27]. The following criteria were established to ensure reasonable values for the azimuthally averaged winds in each belt. If any of the conditions below were not met, a missing value was assigned:

- (1) The number of available data points for each belt must exceed 5.
- (2) The proportion of available data points in each annular belt must be larger than 50%.

Then, the tangential wind speed v_θ was assumed to follow the Rankine vortex:

$$v_\theta(r) = Cr^{-b} \quad (1)$$

where v_θ is the tangential wind speed, r is the radial distance from the TC center, and C and b are constants for a given profile. Due to the similarity between tangential and total winds, especially at radii far away from the maximum wind radius where the radial wind speed is small [28], the total wind was assumed to be the same as the tangential wind. After taking logarithms, the profile in equation (1) was fitted using six azimuthally averaged winds closest to 34 knots. It should be noted that the R34 value in (1) is considered acceptable only when the innermost azimuthally averaged wind is ≥ 34 knots. In other words, extrapolation of TC size is not allowed.

3. Results

3.1. R34 Point-To-Point Comparison between CMA and JTWC Datasets

Figure 2 illustrates a point-to-point comparison between CMA and JTWC size data. It can be observed that these two datasets exhibit a strong correlation, with a correlation coefficient of 0.71. In the CMA dataset, the maximum TC size is 372 km, the minimum is 70.9 km, and the average TC size is 174.3 km. Similarly, for the JTWC dataset, the maximum TC size is 481.5 km, the minimum is 27.8 km, and the average TC size is 197.1 km, indicating a relatively close match between the statistics of the two datasets. However, there is a notable deviation between individual data points from the two datasets. The maximum

deviation is 240.4 km, with an average deviation of 48.6 km. Furthermore, concerning larger TC sizes (approximately greater than 150 km), the JTWC's R34 values tend to be larger than those of the CMA. Conversely, for smaller TC sizes (approximately less than 150 km), the JTWC's R34 values are often smaller than the CMA's. This observation aligns with a study conducted by Kim et al. [24], which discovered a similar trend in the R50 values between the JTWC and KMA datasets. This may be because larger (smaller) TCs typically have higher (lower) intensity [29], and the JTWC reports larger TC intensities compared to the CMA [30]. Therefore, the JTWC's algorithm for estimating TC size is likely related to TC intensity. For larger tropical cyclone sizes, the JTWC's R34 values tend to be larger than those of the CMA.

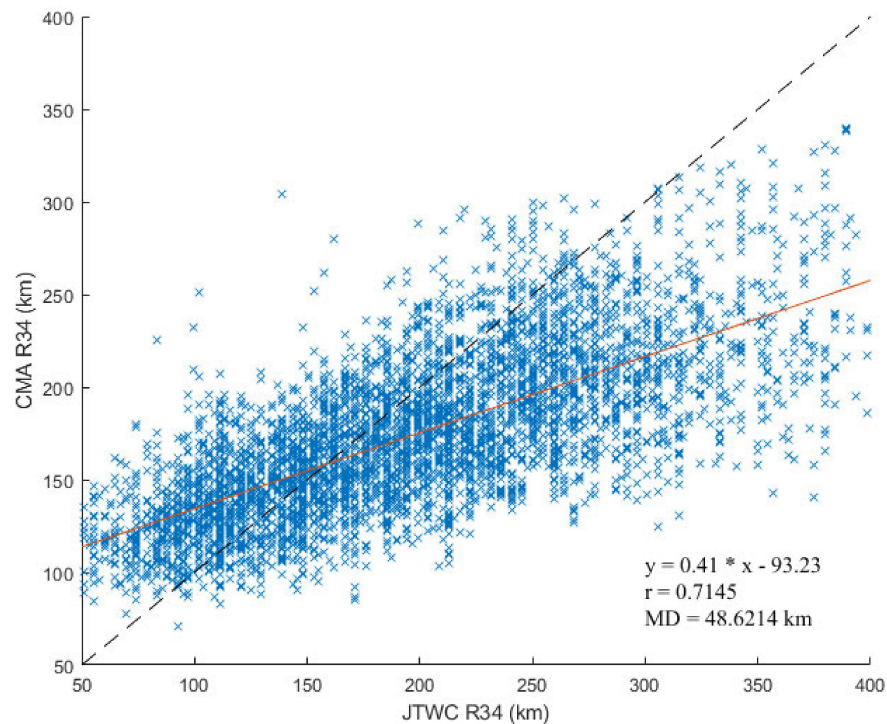


Figure 2. Point-to-point comparison between CMA and JTWC size data. The linear regression equation, the correlation coefficient (r), and the mean deviation (MD) are shown in the bottom right corner.

3.2. The Spatial Distribution Characteristics of R34 from CMA and JTWC Datasets

To compare the spatial distribution of the R34 estimated by two agencies, we first grouped the R34 data into $2^\circ \times 2^\circ$ grids. Following the approach suggested by Kim et al. [24], we then utilized a $4^\circ \times 4^\circ$ moving window to calculate the average R34 values from both agencies. The primary objective of this approach was to minimize the potential impact of spatially variable outliers on the overall analysis. The resulting spatial distributions of R34 from the CMA and JTWC datasets are depicted in Figure 3. Notably, significant differences between the two datasets can be observed in the magnitude of R34 values. The average R34 radius for the CMA is approximately 220 km, whereas the JTWC reaches up to 280 km. However, despite these differences, their spatial distribution has a notable similarity, with a spatial correlation coefficient of 0.61.

In terms of longitudinal distribution, there is a region of smaller R34 values to the east of 120° E, a region of larger R34 values between 120° E and 150° E, and another region of smaller R34 values to the east of 150° E. As for the latitudinal distribution, there is a region of higher R34 values near 25° N, which aligns with the findings of Chan and Chan [18] and Chan and Chan [31]. These findings are also consistent with Lu's [25] research, which suggests that TC size exhibits regional variations, with larger-sized TCs often occurring near the Korean Peninsula and southwestern Japan. Furthermore, Evans et al. have proposed

that TC size, as indicated by R34, tends to increase during the extratropical transition, particularly when TCs approach or cross the latitude of 30° N, denoting the transition from tropical to extratropical regions. During this transition, TCs may undergo structural and characteristic changes influenced by atmospheric circulation systems at higher latitudes. By considering both longitudinal and latitudinal variations, it can be inferred that the spatial variation in size corresponds to the typical east-to-west and south-to-north movement of TCs during the development stage [32].

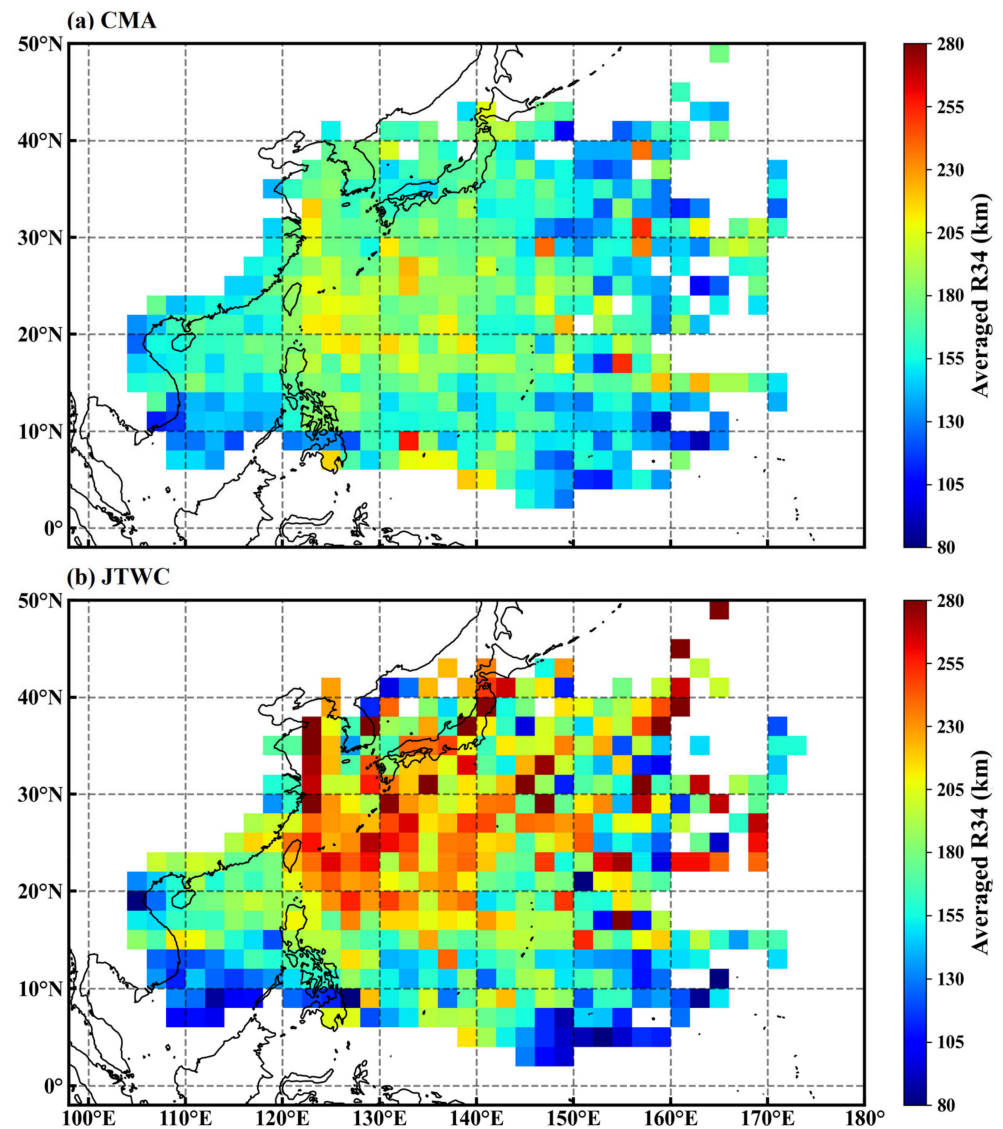


Figure 3. Comparison of the spatial distribution of $2^{\circ} \times 2^{\circ}$ R34 values for (a) CMA and (b) JTWC from 2001 to 2016.

Figure 4 presents the spatial distribution of the difference in $2^{\circ} \times 2^{\circ}$ R34 values between the CMA and JTWC. A noticeable characteristic is that the difference values in R34 between the two datasets tend to decrease as latitude increases. This pattern aligns with the earlier finding in Section 3.1, which indicates that the CMA tends to report larger R34 values for smaller TCs compared to the JTWC. Additionally, it corresponds to the observation that smaller TCs typically form in lower-latitude regions and move northwestward, eventually developing into larger TCs, as shown in Figure 3. Seen from Figure 4, it can be found that below approximately 15° N, the CMA generally reports larger R34 values than JTWC. However, above 25° N, the situation reverses, and the JTWC's R34 values tend to be larger

than those reported by the CMA. In the intermediate region between 15° N and 25° N, the differences in R34 values between the two datasets are relatively small.

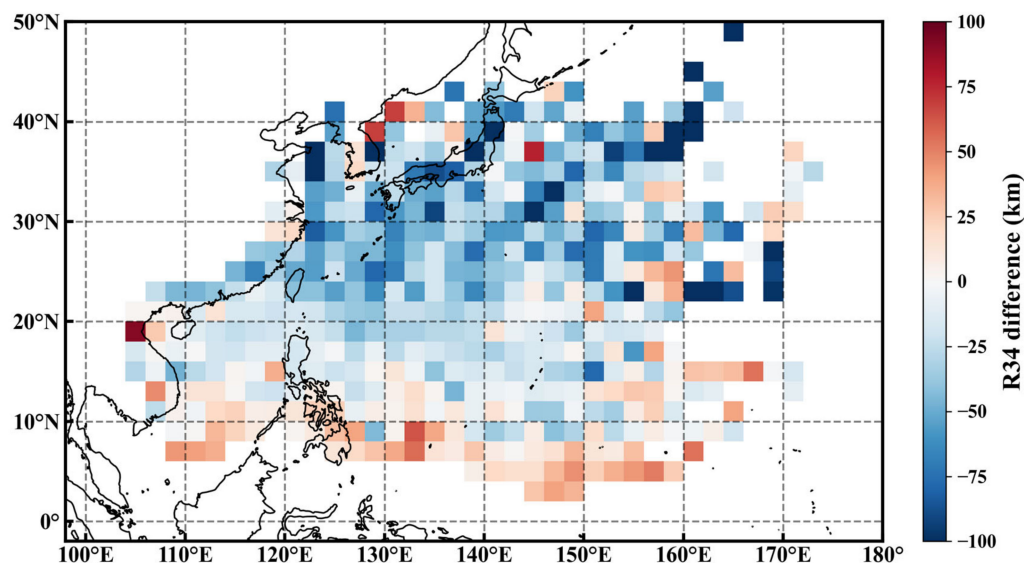


Figure 4. Spatial distribution of the difference in $2^\circ \times 2^\circ$ R34 values between CMA and JTWC from 2001 to 2016.

3.3. The Relationship of R34 Difference with R34, Vmax, SLP, and Latitude

To better understand the differences between the CMA’s and JTWC’s R34 datasets, we studied the correlation between R34 differences and four key parameters, including the size indicator, R34; the TC intensity indicator, maximum wind speed Vmax; the sea-level pressure, SLP; as well as the spatial indicator, latitude. The correlation coefficients based on all data points can be seen in Table 1. The results show that there is the strongest correlation between R34 differences and R34 values, with a correlation of up to 0.58 with the JTWC’s R34 values. This is consistent with the conclusion in Section 3.1, which states that compared to the JTWC, the CMA tends to underestimate large R34 values and overestimate small R34 values. In addition, there is a significant correlation between R34 differences and latitude, with a correlation of 0.26 in both the CMA and JTWC datasets. This also aligns with the conclusion in Section 3.2, which indicates a quasi-linear trend of R34 differences shifting from positive to negative with latitude. Furthermore, R34 differences show no significant correlation with the intensity indicators Vmax and SLP, with correlation coefficients close to 0 for both CMA and JTWC datasets. In fact, there are significant differences in TC intensity between the JTWC and CMA datasets. A study showed that the correlation coefficient between Vmax for the CMA and JTWC datasets during the period from 1981 to 2016 was only 0.487 [33,34]. Additionally, research has also shown a weak correlation between TC intensity and TC size [10,25], which contributes to the weak correlation between R34 differences and intensity indicators here.

Table 1. The correlation coefficients between R34 differences and R34, Vmax, SLP, and latitude in the two datasets.

The Parameters Are Correlated with the Discrepancies in R34	R34	VAMX	SLP	Latitude
CMA	0.16	0.05	−0.06	0.26
JTWC	0.58	0.01	−0.01	0.26

To determine the range of significant discrepancies in four parameters (Vmax, SLP, R34, and latitude) influencing the size of TCs within the R34 estimations of the JTWC, the parameters were compared at intervals of 5 m/s, 15 hPa, 50 km, and 5° , respectively (Figure 5).

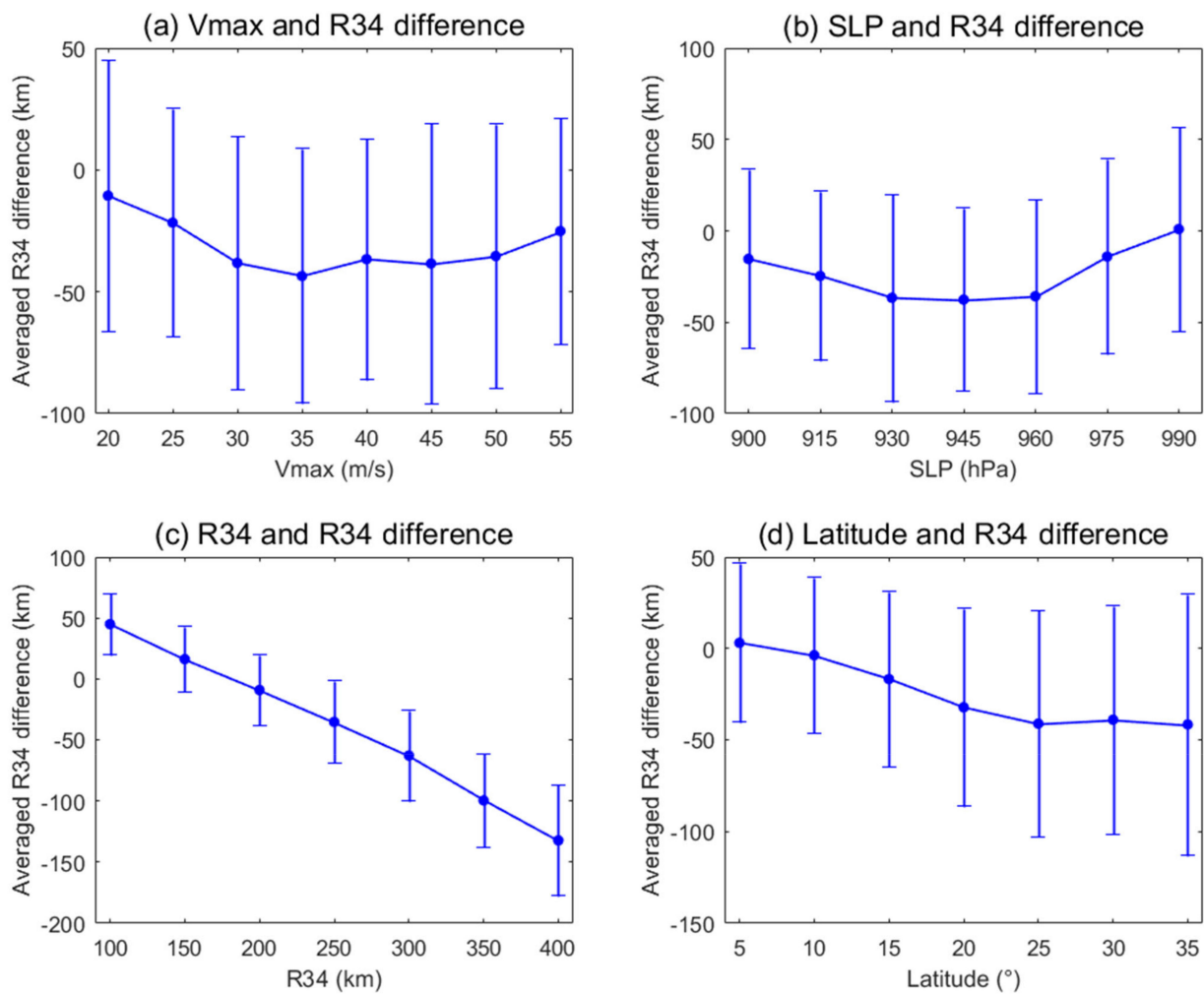


Figure 5. The comparison of R34 difference between CMA and JTWC concerning (a) Vmax, (b) SLP, (c) R34, and (d) latitude, showing the average values (circles) and standard deviations (error bars) in each bin. Bins were defined using $5 \text{ m}\cdot\text{s}^{-1}$ intervals for Vmax, 15 hPa for SLP, 50 km for R34, and 5° for latitude.

Regarding Vmax (Figure 5a), the average R34 difference between the CMA and JTWC is negative, with overall changes in average R34 difference remaining relatively small as Vmax increases. Regarding SLP (Figure 5b), the average R34 difference between the CMA and JTWC fluctuates slightly within the 975–990 hPa range, with overall changes in average R34 difference remaining relatively small as SLP increases. Consistent with previous conclusions, the differences in R34 datasets between the two agencies are unrelated to Vmax and SLP.

Regarding R34 values (Figure 5c), as R34 increases, the average R34 difference shows a linear decrease. When R34 is less than 200 km, the average R34 difference is positive, indicating that the CMA's R34 values on average are larger than those of the JTWC for smaller-sized typhoons. Beyond 200 km, the average R34 difference becomes negative and increases with increasing R34. This suggests that for larger-sized typhoons, the CMA's R34 values on average are smaller than those of the JTWC, and as the size of the typhoon increases, the differences in typhoon R34 values between the two agencies also become larger. This is consistent with the conclusion in Section 3.1 that for larger R34 values, the JTWC tends to report higher values than the CMA, while for smaller R34 values, the opposite is true. Thus, significant discrepancies exist between the two agencies in terms of the storm radius of larger-sized typhoons.

Regarding latitude (Figure 5d), a quasi-linear trend of R34 difference shifting from positive to negative with latitude is observed, consistent with the conclusion in Section 3.2. Below approximately 15° N, the CMA typically reports larger R34 values than the JTWC. However, above 25° N, the situation is reversed, with the JTWC's R34 values often being larger than those reported by the CMA. In the intermediate region between 15° N and 25° N, the differences in R34 values between the two datasets are relatively small. Therefore, significant discrepancies exist between the two agencies in terms of latitude. This could be due to the fact that the CMA and JTWC employ distinct methodologies and consider different parameters when estimating TC wind radii. These methodological distinctions may become more prominent in mid- to high-latitude regions, where the climatic and oceanic conditions can accentuate the discrepancies in the models and methodologies used by both agencies. Mid- to high-latitude regions' climatic and environmental characteristics are likely to influence the data analysis conducted by both agencies significantly. Variations in climate and oceanic conditions in these areas, such as sea surface temperatures and wind field characteristics, can have a pronounced impact on the development and structure of TCs, thus affecting the estimation of R34. For example, the central area of the South China Sea, extending from the east of Luzon Island to the southeast of Taiwan Island, witnesses the highest frequency of TC activity, with active centers located at different positions. These regions with a high frequency of TCs fall within the Western Pacific Warm Pool, which is conducive to developing TCs. The CMA's data results suggest a higher frequency of TC activity in the central South China Sea. In comparison, the JTWC's data results indicate a higher frequency of TC activity east of Luzon Island to the southeast of Taiwan Island [34]. In mid-latitude regions, the paths and intensities of TCs can undergo significant variations, potentially leading to discrepancies in the two agencies' analysis and prediction of these TCs. For example, when TCs approach or pass through mid-latitude areas, they may undergo structural changes due to interactions with temperate airflows.

3.4. Case Study Based on Satellite Data

As indicated in Lu et al. [25], the algorithm used to produce the CMA R34 dataset is based on the reference value of JTWC R34, suggesting a certain correlation between these two datasets. To better understand the differences between these two R34 datasets, we selected two cases with satellite data coverage and obtained R34 values directly through satellite data. The R34 values obtained from the satellite are independent of both CMA and JTWC datasets, enabling a more objective analysis of the disparities in CMA and JTWC R34 datasets.

3.4.1. Case Study of Typhoon "Danasis"

The first case is Typhoon "Danasis" in 2013. This typhoon formed on 1 October 2013, strengthened to a category 4 typhoon on 7 October, and weakened into an extratropical cyclone on 9 October. Here, a period with good satellite data coverage (from 2 October UTC 12:00 to 6 October UTC 12:00) was chosen for calculating R34. Figure 6 displays the distribution of 10 m wind fields from ASCAT at four different time points during this period, along with the calculated R34 based on ASCAT data. The figure shows that the satellite wind speed data coverage is satisfactory throughout the selected period, and the R34 calculated by ASCAT demonstrates high reliability. Additionally, Figure 6 illustrates that ASCAT's R34 aligns well with the R34 datasets from the CMA and JTWC, although there are occasional significant differences between them.

The variations in the three R34 values over time are shown in Figure 7. It can be observed that prior to 2 October, 18:00 UTC, the R34 values from the two agencies and the calculated R34 values from satellite data are similar, ranging from 150 to 200 km. Afterward, the R34 values from ASCAT and JTWC sharply increase, while the increase in the CMA's R34 is relatively small. By 4 October, 12:00 UTC, ASCAT's R34 and JTWC's R34 exceed 300 km, whereas the CMA's R34 is less than 250 km. From 5 October, 18:00 UTC to 6 October, 18:00 UTC, ASCAT's R34 slightly increases, the JTWC's R34 remains unchanged, and the

CMA's R34 slightly decreases. However, between 18:00 UTC on 5 October and 12:00 UTC on 6 October, all three R34 values decrease, with ASCAT's R34 showing a more significant reduction, reaching 200 km by 12:00 UTC on 6 October, which is closer to the CMA's R34. On average, the JTWC's R34 aligns more closely with ASCAT's R34, particularly capturing the rapid increase in size from 3 October to 4th. However, the JTWC's R34 fails to capture the sharp decrease in size on 6 October. Therefore, ultimately, the CMA's R34 is closer to ASCAT's R34. These characteristics may be attributed to the JTWC's use of the Dvorak method [35], which tends to capture the intensification process of typhoons during their development stages [36]. The CMA, on the other hand, did not accurately capture the rapid growth in typhoon size. As a result, there was a significant underestimation of typhoon size afterward. This observation aligns with the findings discussed in Section 3.1, where it was indicated that the CMA dataset typically underestimates larger typhoon sizes.

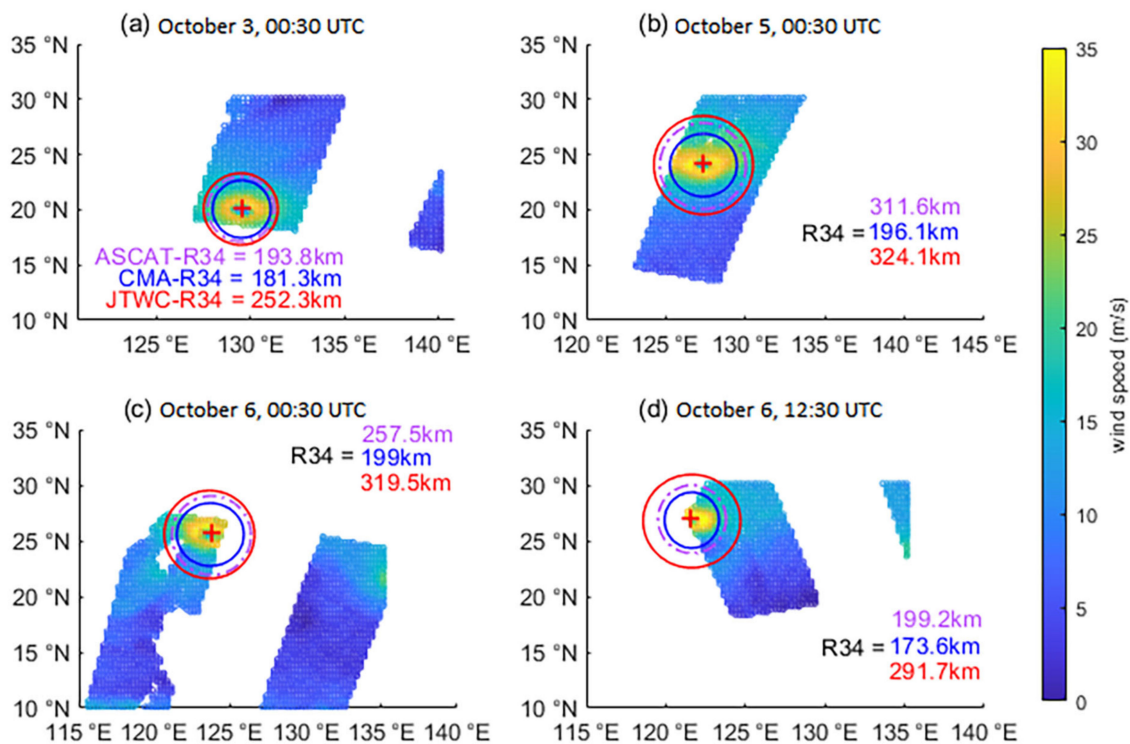


Figure 6. The ASCAT 10 m wind field for Typhoon “Danasis” at four different time points, along with ASCAT R34 (purple circle), CMA R34 value (blue circle), and JTWC R34 value (red circle): (a) October 3 00:30 UTC, (b) October 5 00:30 UTC, (c) October 6 00:30 UTC, and (d) October 6 12:30 UTC. The red cross indicates the center of the TC.

3.4.2. Case Study of Typhoon “Maysak”

In the case study of Typhoon “Danas”, only the intensifying period is considered due to the availability of satellite data. To investigate how the R34 values estimated by the two agencies behave during the decaying stage of TCs, the second case study focuses on Typhoon “Maysak” in 2015. In this case, satellite data cover almost the entire decaying period of the typhoon, from 31 March at 00:00 UTC to 4 April at 18:00 UTC. Typhoon “Maysak” formed on 28 March UTC 03:00, 2015. It continued to intensify and reached super typhoon status on 31 March UTC 20:00. Subsequently, it gradually weakened and made landfall in the Philippines on 5 April UTC 11:00, downgrading to a tropical depression. Figure 8 illustrates the distribution of 10 m wind fields from ASCAT at four different time points during this period. The extensive coverage of satellite data ensures the reliability of the R34 values calculated from ASCAT. Furthermore, Figure 8 indicates that the three types of R34 data are consistent with each other, exhibiting only minor differences.

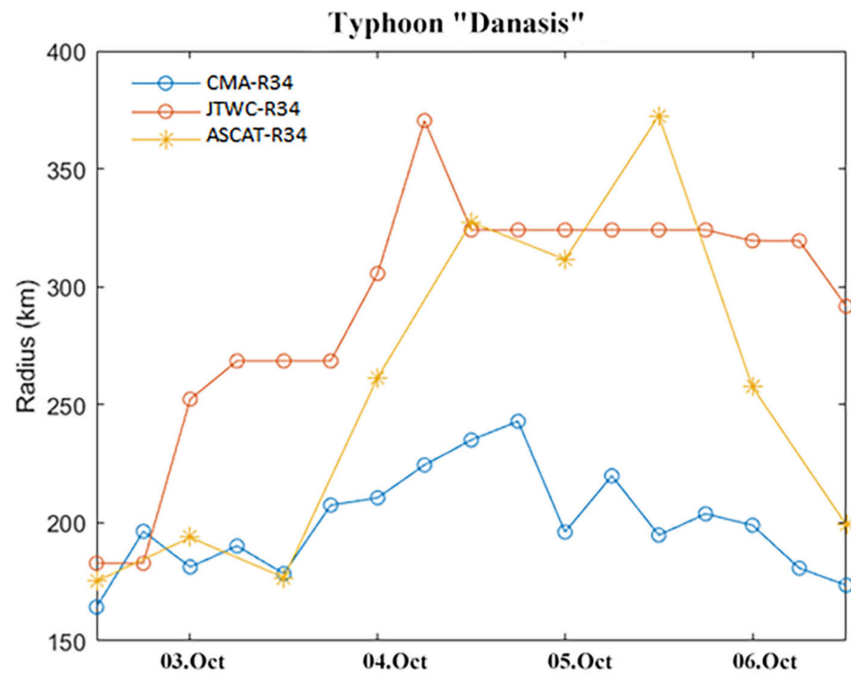


Figure 7. For Typhoon "Danasis", the estimated R34 values by CMA (in blue), JTWC (in orange), and ASCAT (in yellow) are every 6 h from 12:00 on 2 October to 12:00 on 6 October.

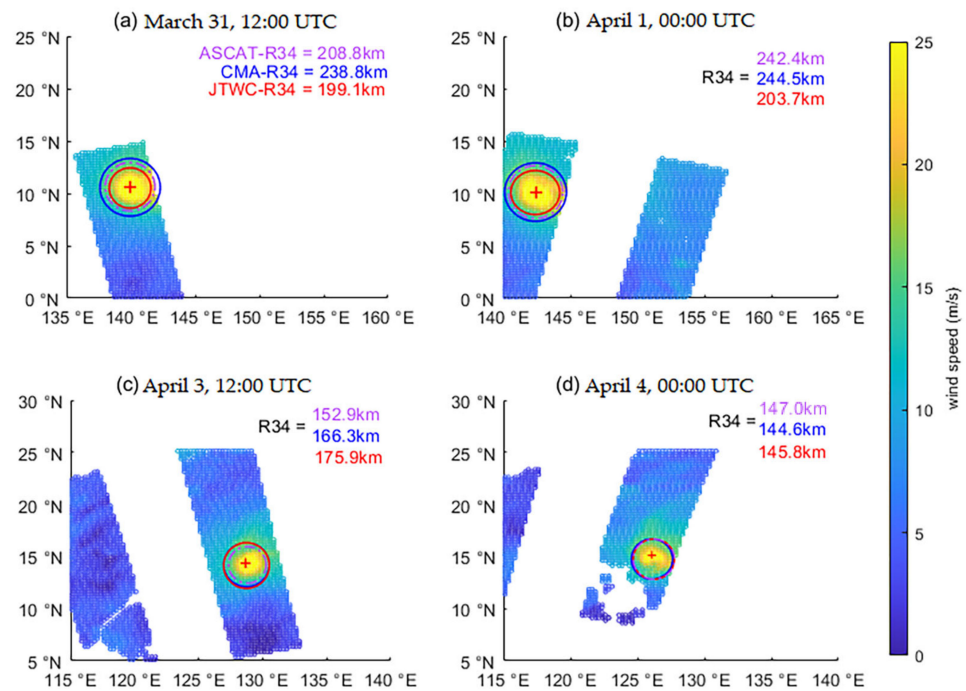


Figure 8. Same as Figure 6, but for Typhoon 'Maysak': (a) 12:00 UTC on 31 March, (b) 00:00 UTC on 1 April, (c) 12:00 UTC on 3 April, and (d) 00:00 UTC on 4 April.

Figure 9 shows the time-varying R34 values from the three sources; it can be observed that the trend of R34 values from both the CMA and JTWC decreases gradually. After 00:00 UTC on 31 March, as the typhoon weakens, the discrepancy between the CMA's and JTWC's R34 values gradually increases, with the intensity of the TC at this time of Severe Tropical Storm (ST). By 00:00 UTC on 1 April, the CMA's R34 value reached its maximum, similar to the satellite-estimated R34 value. After 06:00 UTC on 1 April, as the typhoon weakened, the R34 values from both agencies started to decrease rapidly. After

00:00 UTC on 3 April, the R34 values from both agencies become close and are similar to the satellite-estimated R34 value. At this time, the intensity of the TC is Typhoon (TY), and after 00:00 UTC on 4 April, the TC weakens to Tropical Storm (TS). This indicates that during the decay stage of TCs, as the TC size decreases, the R34 values estimated by both agencies perform well. On the one hand, the good coverage of satellite data was utilized by both agencies for this typhoon. Additionally, research [37] indicates that QuikSCAT ocean surface wind data can effectively rectify positioning and intensity discrepancies of tropical cyclones, particularly weak ones, reflecting the distribution of the cyclonic wind field and the lower-level environmental flow field. On the other hand, as observed from Figure 8, during the typhoon's weakening phase, the distribution of the typhoon's wind field exhibits good symmetry, indicating a more stable typhoon system with a more intact storm structure, thereby resulting in better performance of R34 values from both agencies.

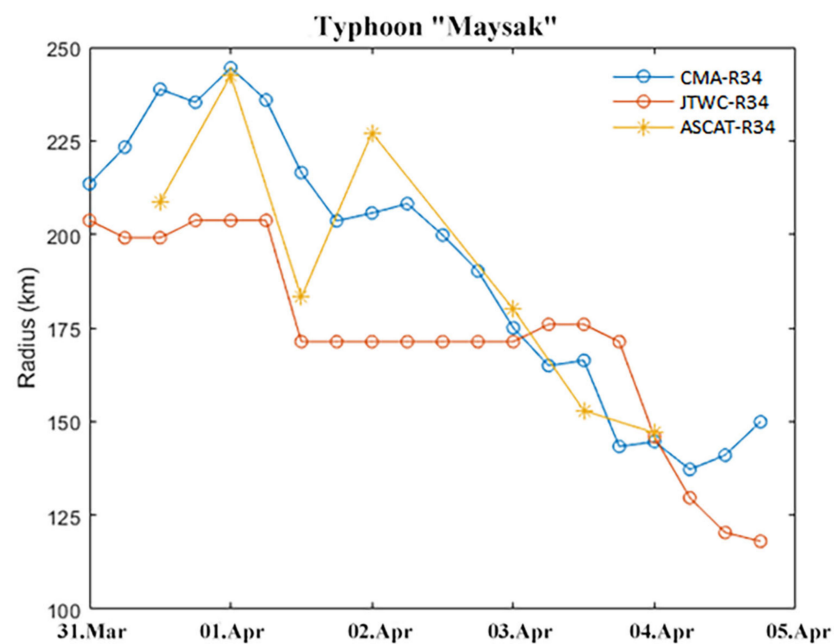


Figure 9. For Typhoon "Maysak", the estimated R34 values by CMA (in blue), JTWC (in orange), and ASCAT (in yellow) every 6 h from 00:00 on 31 March to 00:00 on 5 April.

4. Discussion

TC size is a critical factor in predicting disasters caused by TCs. The CMA and JTWC provide critical data for forecasting typhoon disasters, particularly regarding TC size data. However, a detailed investigation into the specific features of TC size estimated by these two agencies has not been conducted. This study aims to investigate the characteristics of R34 estimated by two agencies. Its objectives include examining the correlation between the two datasets, analyzing their spatial distribution features, and investigating key parameters affecting R34 estimations.

Firstly, a point-to-point comparison of size data from both agencies shows a strong correlation between the two datasets, with a correlation coefficient of 0.71. In the CMA dataset, the maximum size of a typhoon is 372 km, the minimum is 70.9 km, and the average size is 174.3 km. Similarly, in the JTWC dataset, the maximum size is 481.5 km, the minimum is 27.8 km, and the average size is 197.1 km, indicating relatively close statistical data between the two datasets. Lu's [38] research indicates that TCs in the WNP region have an average size of 203 km, with larger sizes observed for stronger TCs. Additionally, studies [39] suggest that scatterometer-based data, used as a reference, indicate that the JTWC provides higher TC intensities compared to the JMA and CMA. Therefore, for larger typhoon sizes (approximately greater than 150 km), the JTWC's R34 values tend to be larger than those

of the CMA. Conversely, for smaller typhoon sizes (approximately less than 150 km), the JTWC's R34 values are often smaller than the CMA's.

Secondly, by comparing the spatial distribution of the R34 estimates from the two agencies, significant discrepancies in R34 values between the two datasets are observed. The average R34 value for the CMA is approximately 220 km, while the JTWC's R34 value can reach up to 280 km. However, despite these discrepancies, their spatial distributions still exhibit significant similarity, with a spatial correlation coefficient of 0.61. In terms of longitudinal distribution, smaller R34 values are observed to the east of 120° E, larger R34 values are found between 120° E and 150° E, and smaller R34 values again appear to the east of 150° E. As for the latitudinal distribution, higher R34 values are observed near 25° N. This aligns with Lu's [38] research findings, which observed that regional tropical cyclone (TC) distributions indicate the largest mean size (250–280 km) for TCs affecting southwestern Japan. By comparing the spatial distribution of R34 value differences estimated by the two agencies, it was observed that the differences in R34 values between the CMA and JTWC tend to decrease as latitude increases.

Furthermore, the impact of four key parameters related to TC size (V_{max} , SLP, latitude, and R34) on the R34 estimations of the two agencies was investigated. The strongest correlation was found between R34 difference and R34 values, with a high correlation of up to 0.58 with the JTWC's R34 values. There was also a significant correlation between R34 difference and latitude, with a correlation coefficient of 0.26 in both the CMA and JTWC datasets. However, the R34 difference showed no significant correlation with the intensity indicators V_{max} and SLP, with correlation coefficients close to 0 in both the CMA and JTWC datasets.

Lastly, through case studies of two different development stages of Typhoons "Danas" and "Maysak", the distinct characteristics of R34 estimations by the two agencies during different TC development stages were confirmed. During the typhoon development stage, the JTWC tends to capture the intensification process of the typhoon more accurately, reflecting the size changes during the typhoon's strengthening process. The CMA failed to accurately capture the rapid growth in typhoon size, resulting in a significant underestimation of typhoon size. During the typhoon weakening stage, as the typhoon's size decreases, the R34 values estimated by both agencies perform well. This could be attributed to the fact that a tropical cyclone (TC) tends to reach its maximum size 6 h after it reaches its maximum intensity, and the rate of size decrease during the weakening stage of a TC is much smaller than the rate of size increase during its development stage [30].

5. Conclusions

This study provides quantitative information on the characteristics and discrepancies of the R34 datasets between the CMA and JTWC. The results show that the statistical data of the R34 datasets between the CMA and JTWC are relatively close, but there are regional variations in their spatial distribution. These discrepancies mainly arise from each agency's specific estimation methods to calculate the R34 values due to the parameters primarily considered by the two agencies when estimating the TC size. Research has shown that differences in data between different organizations are caused by varying algorithms used in weather services to estimate TCs [24,39]. Overall, the discrepancies between the Northwestern Pacific TC datasets of the CMA and JTWC are pronounced, and each has its distinct characteristics. At this juncture, determining the optimal policy or the most reliable wind radius estimation method remains to be discovered, as each agency has established its policies based on distinct objectives. Nonetheless, these policy variations contribute to the uncertainty and inconsistency in TC size data, rendering them unsuitable for research. This stands in contrast to earlier studies that asserted the reliability of wind radii in best-track data [40,41]. Consequently, researchers must be cognizant of the distinct characteristics of wind radius estimations from each agency and judiciously select and employ the data aligning with the objectives of their respective studies. This study furnishes valuable insights for facilitating such informed choices. Moreover, the findings can serve as a foundational framework for devising a method that ensures consistent wind radius

estimations across diverse agencies. However, there are several notable limitations and shortcomings that should be acknowledged. This study acknowledges that discrepancies in data between different organizations are attributed to varying algorithms used in weather services to estimate TCs. However, it does not thoroughly explore the specific algorithms employed by the CMA and JTWC, nor does it assess the impact of these algorithms on the accuracy and reliability of the R34 datasets.

Author Contributions: Conceptualization, J.L. and Y.L.; methodology, Y.L.; software, J.L.; validation, J.L. and Y.L.; formal analysis, J.L.; investigation, J.L. and J.T.; resources, J.L.; data curation, J.L.; writing—original draft preparation, J.L.; writing—review and editing, Y.L. and J.T.; visualization, J.L.; supervision, Y.L.; project administration, Y.L. and J.T.; funding acquisition, Y.L. and J.T. All authors have read and agreed to the published version of the manuscript.

Funding: This research was funded by the National Natural Science Foundation of China, grant number 42075072.

Institutional Review Board Statement: Not applicable.

Informed Consent Statement: Not applicable.

Data Availability Statement: Publicly available datasets were analyzed in this study. These data can be found here: CMA data are available at <http://www.tcdata.typhoon.org.cn> (accessed on 20 December 2022); JTWC data are available at <https://www.metoc.navy.mil/jtwc/jtwc.html?western-pacific> (accessed on 20 December 2022); ASCAT data are available at <http://www.knmi.nl/scatterometer/ascatsos12prod/> (accessed on 15 July 2022).

Acknowledgments: The numerical calculations in this paper have been done on the supercomputing system in the Supercomputing Center of Nanjing University of Information Science & Technology.

Conflicts of Interest: The authors declare no conflicts of interest.

References

1. Wang, H.; Xu, M.; Onyejuruwa, A.; Wang, Y.; Wen, S.; Gao, A.E.; Li, Y. Tropical cyclone damages in Mainland China over 2005–2016: Losses analysis and implications. *Environ. Dev. Sustain.* **2019**, *21*, 3077–3092. [CrossRef]
2. Schmidt, S.; Kemfert, C.; Höpfe, P. The impact of socio-economics and climate change on tropical cyclone losses in the USA. *Reg. Environ. Change J.* **2010**, *10*, 13–26. [CrossRef]
3. Liu, D.; Pang, L.; Xie, B. Typhoon disaster in China: Prediction, prevention, and mitigation. *Nat. Hazards* **2009**, *49*, 421–436. [CrossRef]
4. Knaff, J.A.; Sampson, C.R.; Chirokova, G. A global statistical–dynamical tropical cyclone wind radii forecast scheme. *Weather Forecast.* **2017**, *32*, 629–644. [CrossRef]
5. Chan, J.C.L.; Yip, C.K.M. Interannual variations of tropical cyclone size over the western North Pacific. *Geophys. Res. Lett.* **2003**, *30*, 2267. [CrossRef]
6. Kimball, S.K.; Mulekar, M.S. A 15-year climatology of North Atlantic tropical cyclones. Part I: Size parameters. *J. Clim.* **2004**, *17*, 3555–3575. [CrossRef]
7. Zhan, R.; Wang, Y. Weak tropical cyclones dominate the poleward migration of the annual mean location of lifetime maximum intensity of Northwest Pacific tropical cyclones since 1980. *J. Clim.* **2017**, *30*, 6873–6882. [CrossRef]
8. Knaff, J.A.; Sampson, C.R.; DeMaria, M.; Marchok, T.P.; Gross, J.M.; McAdie, C.J. Statistical tropical cyclone wind radii prediction using climatology and persistence. *Weather Forecast.* **2007**, *22*, 781–791. [CrossRef]
9. Merrill, R.T. A comparison of large and small tropical cyclones. *Mon. Weather Rev.* **1984**, *112*, 1408–1418. [CrossRef]
10. Lungu, T.; Callahan, P.S. Quikscat Science Data Product User’s Manual: Overview and Geophysical Data Products, Jet Propulsion Laboratory. D-18053-Rev A, version 3. 2006, p. 91. Available online: http://web.eng.ucsd.edu/~sgls/final_galley.pdf (accessed on 3 March 2024).
11. Bentamy, A.; Croize-Fillon, D.; Perigaud, C. Characterization of ASCAT measurements based on buoy and QuikSCAT wind vector observations. *Ocean Sci.* **2008**, *4*, 265–274. [CrossRef]
12. Sampson, C.R.; Goerss, J.S.; Knaff, J.A.; Strahl, B.R.; Fukada, E.M.; Serra, E.A. Tropical cyclone gale wind radii estimates, forecasts, and error forecasts for the Western North Pacific. *Weather Forecast.* **2018**, *33*, 1081–1092. [CrossRef]
13. Knapp, K.R.; Kruk, M.C.; Levinson, D.H.; Diamond, H.J.; Neumann, C.J. The international best track archive for climate stewardship (IBTrACS). *Bull. Am. Meteorol. Soc.* **2010**, *91*, 363–376. [CrossRef]
14. Knaff, J.A.; Sampson, C.R.; Kucas, M.E.; Slocum, C.J.; Brennan, M.J.; Meissner, T.; Ricciardulli, L.; Mouche, A.; Reul, N.; Morris, M.; et al. Estimating tropical cyclone surface winds: Current status, emerging technologies, historical evolution, and a look to the future. *Trop. Cyclone Res. Rev.* **2021**, *10*, 125–150. [CrossRef]

15. Zhao, K.; Zhao, C. Evaluation of HY-2a scatterometer ocean surface wind data during 2012–2018. *Remote Sens.* **2019**, *11*, 2968. [[CrossRef](#)]
16. Lee, C.-S.; Cheung, K.K.W.; Fang, W.-T.; Elsberry, R.L. Initial maintenance of tropical cyclone size in the Western North Pacific. *Mon. Weather Rev.* **2010**, *138*, 3207–3223. [[CrossRef](#)]
17. Misra, T.; Chakraborty, P.; Lad, C.; Gupta, P.; Rao, J.; Upadhyay, G.; Kumar, S.V.; Kumar, B.S.; Gangele, S.; Sinha, S.; et al. SCATSAT-1 scatterometer: An improved successor of OSCAT. *Curr. Sci.* **2019**, *117*, 941–949. [[CrossRef](#)]
18. Chan, K.T.F.; Chan, J.C.L. Size and strength of tropical cyclones as inferred from QuikSCAT data. *Mon. Weather Rev.* **2012**, *140*, 811–824. [[CrossRef](#)]
19. Knaff, J.A.; DeMaria, M.; Molenar, D.A.; Sampson, C.R.; Seybold, M.G. An automated, objective, multiple-satellite-platform tropical cyclone surface wind analysis. *J. Appl. Meteorol. Clim.* **2011**, *50*, 2149–2166. [[CrossRef](#)]
20. Hong, S.; Shin, I. Wind speed retrieval based on sea surface roughness measurements from spaceborne microwave radiometers. *J. Appl. Meteorol. Clim.* **2013**, *52*, 507–516. [[CrossRef](#)]
21. Kwon, M. Estimation and statistical characteristics of the radius of maximum wind of tropical cyclones using COMS IR imagery. *Atmosphere* **2012**, *22*, 473–481. [[CrossRef](#)]
22. Lee, Y.-K.; Kwon, M. An estimation of the of tropical cyclone size using COMS infrared imagery. *Atmosphere* **2015**, *25*, 569–573. [[CrossRef](#)]
23. Song, J.; Klotzbach, P.J. Wind structure discrepancies between two best track datasets for Western North Pacific tropical cyclones. *Mon. Weather Rev.* **2016**, *144*, 4533–4551. [[CrossRef](#)]
24. Kim, H.-J.; Moon, I.-J.; Oh, I. Comparison of tropical cyclone wind radius estimates between the KMA, RSMC Tokyo, and JTWC. *Asia-Pac. J. Atmos. Sci.* **2022**, *58*, 563–576. [[CrossRef](#)]
25. Lu, X.; Yu, H.; Yang, X.; Li, X. Estimating tropical cyclone size in the northwestern pacific from geostationary satellite infrared images. *Remote Sens.* **2017**, *9*, 728. [[CrossRef](#)]
26. Yu, H.; Hu, C.; Jiang, L. Comparison of three tropical cyclone intensity datasets. *Acta Meteorol. Sin.* **2007**, *21*, 121.
27. Shea, D.J.; Gray, W.M. The hurricane’s inner core region. I. Symmetric and asymmetric structure. *J. Atmos. Sci.* **1973**, *30*, 1544–1564. [[CrossRef](#)]
28. Sampson, C.R.; Knaff, J.A. A Consensus Forecast for Tropical Cyclone Gale Wind Radii. *Weather Forecast.* **2015**, *30*, 1397–1403. [[CrossRef](#)]
29. Weatherford, C.L.; Gray, W.M. Typhoon structure as revealed by aircraft reconnaissance. Part I: Data analysis and climatology. *Mon. Weather Rev.* **1988**, *116*, 1032–1043. [[CrossRef](#)]
30. Wu, L.; Lei, X. Preliminary research on the size of inner core and periphery and their relationship with the intensity of tropical cyclones. *J. Trop. Meteorol.* **2012**, *28*, 719–725. [[CrossRef](#)]
31. Chan, K.T.F.; Chan, J.C.L. Global climatology of tropical cyclone size as inferred from QuikSCAT data. *Int. J. Clim.* **2015**, *35*, 4843–4848. [[CrossRef](#)]
32. Knaff, J.A.; Longmore, S.P.; Molenar, D.A. An objective satellite-based tropical cyclone size climatology. *J. Clim.* **2014**, *27*, 455–476. [[CrossRef](#)]
33. Song, J.; Wang, Y.; Wu, L. Trend discrepancies among three best track data sets of western North Pacific tropical cyclones. *J. Geophys. Res. Atmos.* **2010**, *115*, D12128. [[CrossRef](#)]
34. Zhang, D.; Zhang, H.; Cheng, X. Comparative analysis on the characteristics of tropical-cyclone activities over the western North Pacific in three datasets. *J. Mar. Sci.* **2020**, *38*, 48–57. [[CrossRef](#)]
35. Dvorak, V.F. *Tropical Cyclone Intensity Analysis Using Satellite Data*; US Department of Commerce, National Oceanic and Atmospheric Administration, National Environmental Satellite, Data, and Information Service: Silver Spring, MD, USA, 1984; Volume 11.
36. Velden, C.; Burton, A.; Kuroiwa, K. The first international workshop on satellite analysis of tropical cyclones: Summary of current operational methods to estimate intensity. *Trop. Cyclone Res. Rev.* **2012**, *1*, 469–481. [[CrossRef](#)]
37. Xiang, F.; Di, X.; Xiaolong, L.; Xin, W. The ocean surface vector wind data of QuikSCAT and its application in tropical cyclone analysis. *Meteorol. Mon.* **2007**, *33*, 33–39.
38. Lu, X.; Yu, H.; Lei, X. Statistics for size and radial wind profile of tropical cyclones in the western North Pacific. *J. Meteorol. Res.* **2011**, *25*, 104–112. [[CrossRef](#)]
39. Barcikowska, M.; Feser, F.; von Storch, H. Usability of best track data in climate statistics in the Western North Pacific. *Mon. Weather Rev.* **2012**, *140*, 2818–2830. [[CrossRef](#)]
40. Knaff, J.A.; Slocum, C.J.; Musgrave, K.D.; Sampson, C.R.; Strahl, B.R. Using routinely available information to estimate tropical cyclone wind structure. *Mon. Weather Rev.* **2016**, *144*, 1233–1247. [[CrossRef](#)]
41. Dolling, K.; Ritchie, E.A.; Tyo, J.S. The use of the deviation angle variance technique on geostationary satellite imagery to estimate tropical cyclone size parameters. *Weather Forecast.* **2016**, *31*, 1625–1642. [[CrossRef](#)]

Disclaimer/Publisher’s Note: The statements, opinions and data contained in all publications are solely those of the individual author(s) and contributor(s) and not of MDPI and/or the editor(s). MDPI and/or the editor(s) disclaim responsibility for any injury to people or property resulting from any ideas, methods, instructions or products referred to in the content.